RADIATIVE DOMINATED COOLING OF THE FLARE CORONA AND TRANSITION REGION

by

S.K. Antiochos

SUIPR Report No. 792

August 1979

INSTITUTE FOR PLASMA RESEARCH
STANFORD UNIVERSITY, STANFORD, CALIFORNIA

RADIATIVE DOMINATED COOLING OF THE FLARE CORONA AND TRANSITION REGION

by

S. K. Antiochos

National Aeronautics and Space Administration
Contracts: NAS8-32263
NGL 05-020-272
NGR 05-020-559

SUIPR Report No. 792

August 1979

Institute for Plasma Research
Stanford University
Stanford, California

ABSTRACT

Recent observations of cooling flare loops indicate that the differential emission measure, Q, of flare coronal and transition region plasma, $T > 10^5$ K, has a much steeper dependence on temperature than in non-flare regions. This result is not compatible with models in which conduction dominates the cooling; hence, we investigate models in which radiation dominates. We find that the radiative models predict $Q \propto T^{\ell+1}$, where ℓ measures the dependence of the radiative loss coefficient on temperature, $\Lambda(T) \sim T^{-\ell}$. We conclude that the radiative models are also incapable of explaining the observations and suggest that large mass motions (velocities of the order of the sound speed) may be required.

I. INTRODUCTION

The high temperature coronal plasma produced by a flare is believed to cool primarily by radiation and conduction to the chromosphere. Since conductive losses increase rapidly with temperature, several authors concluded that conduction dominates radiation, at least during the initial phase when $T \geq 10^7$ K, e.g., Culhane et al. (1970), Moore and Datlowe (1975). However, radiative losses are a strong function of density, and recent EUV and soft x-ray observations have tended to yield increasingly higher density estimates: $n > 10^{11}$ cm^{-3} at $T \approx 10^7$ K, (see Moore et al. 1979). Hence, it appears likely that radiative cooling may dominate in some flares even during the initial cooling phase.

Strong evidence against the dominance of conduction has been obtained from observations of relative line intensities of coronal and transition region lines, i.e. 10^5 K $\leq T \leq 10^7$ K. Given a model for the cooling, the temperature and density profiles and, hence, the emission measure profile (differential emission measure) can be determined. This may then be used to predict relative line intensities which can be compared with the observations. Conductive dominated models have been investigated in detail by Antiochos and Sturrock (1976, 1978). For a plane-parallel isobaric atmosphere the differential emission measure,

$$Q(T) \equiv A\, n^2 \left| \frac{1}{T} \frac{\partial T}{\partial S} \right|^{-1} \tag{1}$$

is related directly to the conductive heat flux,

$$F_c \equiv -\kappa \frac{\partial T}{\partial s} \tag{2}$$

where: A is the area of the emitting region; n is the electron density; $\frac{\partial T}{\partial s}$ is the temperature gradient in the vertical direction; and the conductivity κ is given by Spitzer (1962):

$$\kappa = 10^{-6}\ T^{5/2} \tag{3}$$

Combining (1) - (3) yields:

$$Q(T) = \frac{10^{-6} A p^2}{4k^2}\ T^{3/2} |F_c|^{-1} \tag{4}$$

where the equation of state,

$$p = 2knT \tag{5}$$

has been used.

Antiochos and Sturrock find that for static conductive cooling, $F_c \approx$ const whereas for evaporative conduction $F_c \propto T$. Defining δ as the steepness of the differential emission measure, $Q(T) \propto T^{\delta}$, equation (4) implies that $\delta = 1.5$ for static conduction and $\delta = .5$ for evaporative. Note that these results apply only to a single coronal loop (of constant cross-section), but that the observed emission measure may be due to the contributions of several loops. However, if all the loops are conductively cooling then the observed value of δ must be ≤ 1.5 since no individual loop can have $\delta > 1.5$.

The conductive models are consistant with EUV observations of quiet and active regions which indicate that $\delta \leq 1.5$, e.g., Jordan (1976), Withbroe (1977). However, the models disagree with recent flare observations which imply a very steep dependence of emission measure on temperature. Dere et al. (1977), Dere and Cook (1979), and Widing (1979) find that in three flares $\delta \gtrsim 3.0$ for plasma at $10^{5.5} \lesssim T \lesssim 10^{7}$. Underwood et al. (1978) carried out a detailed comparison of observed line intensities for the 1973 August 9 flare with predictions by the conductive models. By comparing intensities directly they avoided any difficulties with deriving the differential emission measure from the data (Craig and Brown 1976, Underwood and McKenzie 1977). They also found that only models with a large δ, $\gtrsim 3.0$, could be compatible with the data, and that the conductive models were definitely in disagreement. It is difficult to reconcile a large δ with conductive cooling since equation (4) implies that for $\delta > 1.5$ the heat flux actually increases as it passes through the transition region.

Dere and Cook (1979) have attempted to explain their observations as due to the effect of a collection of loops. However, as pointed out previously, no sum of loops can have a differential emission measure steeper than, say $\delta = 1.5$, unless at least one loop has this value or greater. Dere and Cook assume an <u>infinite</u> steepness, i.e., they assume that each loop is perfectly isothermal and, hence, the differential emission measure of each loop is a delta function; but, such a procedure is physically meaningless. Clearly, the temperature profile in each loop must be a continuous function from its maximum value in the corona to its value in the chromosphere, $\sim 10^{4}$ K, and must be determined by the physical processes in the plasma, e.g., conduction and radiation. The point of the observations in that they impose a restriction on the possible form of the temperature

profile and, hence, on the physics of the loop. Dere and Cook have failed to understand this point and have ignored the whole issue by simply assuming an impossible temperature profile.

Underwood et. al. proposed that a possible explanation for the steep profile is that it is due to radiative dominated cooling. The radiative losses are known to be a strong function of temperature and, hence, may be expected to result in the preferential depletion of low temperature plasma over that at higher temperatures. In addition, these authors observe large downward velocities at temperatures where the radiative losses peak, $T \sim 10^5$ K. Downward velocities are also difficult to reconcile with conductive dominated cooling, but they are compatible with the idea that thermal instability creates large pressure gradients which subsequently generate mass motions, (Antiochos 1979).

From the discussion above it appears likely that conductive models are invalid, at least, for some flares. Therefore, in the next section we develop models for the cooling of coronal flare plasma in which radiation dominates and, in particular, we investigate the emission measure profiles that such models predict.

II. MODELS

2.1 Approximations

Assuming a plane-parallel geometry (a loop of constant cross-section), and neglecting gravity, the heat equation can be expressed as:

$$\frac{\partial}{\partial t}\left(3/2p + 1/2\rho v^2\right) + \frac{\partial}{\partial s}\left(1/2\rho v^3 + 5/2pv + F_c\right) = -n^2\Lambda(T) \qquad (6)$$

where: $\Lambda(T)$ is the radiative loss coefficient, e.g., Cox and Tucker 1969; ρ is the mass density; and it is assumed that all flare heating has ended so that there is no energy source term present. (The steady-state coronal heating rate is negligible compared to the energy loss rate of flare plasma.) Simultaneous with (6) the equations of continuity and momentum must be solved. However, the resulting system of equations is sufficiently complex that analytic general solutions are not possible. In addition, numerical simulation is impractical because an extremely fine spatial grid is required to resolve the large temperature gradients expected at lower temperature. Hence, we investigate only certain limiting cases to the complete set of equations.

There are three physical time scales that are relevant to the model; the radiative cooling time

$$\tau_r\ (T) \equiv \frac{3/2p}{n^2\Lambda(T)} \qquad (7)$$

the conductive cooling time,

$$\tau_c\ (T) \equiv \frac{3/2p}{F_c/H(T)} \qquad (8)$$

and the speed of sound propagation time

$$\tau_s\ (T) \equiv \frac{H(T)}{C(T)} \tag{9}$$

where H(T) is the temperature scale height,

$$H(T) = \left|\frac{1}{T}\frac{\partial T}{\partial s}\right|^{-1} \tag{10}$$

and C(T) is the speed of sound. We assume throughout that radiation dominates the cooling,

$$\frac{\tau_r\ (T)}{\tau_c\ (T)} << 1 \tag{11}$$

for T in the range of interest, and hence, the heat flux in equation (6) can be neglected. Two limiting cases can now be defined for the evolution of the flare plasma:

the static $$\frac{\tau_r\ (T)}{\tau_s\ (T)} << 1 \tag{12a}$$

and the isobaric $$\frac{\tau_r\ (T)}{\tau_s\ (T)} >> 1 \tag{12b}$$

In the static case (12a), the radiative cooling is so rapid that even though large pressure gradients are created due to the different cooling rates of plasma at different temperatures, there is insufficient time for large velocities to be generated. Therefore, if the plasma is initially static it will remain so during the cooling phase. In the isobaric case (12b), the speed of sound is so large that mass motions cancel the build up of

pressure gradients so that the plasma is approximately isobaric and all velocities remain small compared to the speed of sound.

Conditions (11) and (12a) or (12b) apply to flares with a high coronal density as in the 1973 August 9 event. Assuming that $\Lambda(T) \approx 10^{-22.5}$ for $T = 10^7$ K yields:

$$\frac{\tau_r}{\tau_c} = 10^{16} \frac{T^{7/2}}{(nH)^2} \tag{13}$$

and

$$\frac{\tau_r}{\tau_s} = 10^{11.3} \frac{T^{3/2}}{(nH)} \tag{14}$$

Hence, for $T = 10^7$ K and $H = 10^{9.8}$ cm, radiation dominates of $n > 10^{10.9}$ cm^{-3}. The isobaric case is valid if $10^{12.5} > n > 10^{10.9}$, whereas the static case holds of $n > 10^{12.5}$ cm^{-3}. However, these numbers are highly variable since equations (13) and (14) indicate that τ_r/τ_c and τ_r/τ_s are sensitive functions of T, n and H, which are not accurately measured. In addition, the plasma parameters vary with time, therefore, each of the radiative cases may be valid only over a limited range of the evolution.

The important points of (13) and (14) are that conditions (11) and (12) are mutually consistant and that both of the radiative cases are possible in view of the uncertainties in T, n and H. Even though neither of the radiative models is complete, much can be gained by examining these simple models before attempting extensive numerical simulations; in particular, it will be possible to determine whether radiative cooling can produce a steep emission measure profile.

2.2 Static Radiative Cooling

Along with assumptions (11) and (12a) initial conditions must be specified

on the plasma profiles. For simplicity, and in order to be consistent with assumptions (12a), we assume that the plasma is initially static and isobaric,

$$v(s,0) = 0 \text{ and } \frac{\partial p}{\partial s}(s,0) = 0 \tag{15}$$

Rather than specifying the initial temperature profile, it is equivalent to specify the initial emission measure profile. This is assumed to be given by the static conductive model of Antiochos and Sturrock 1976:

$$Q_o(T_o) = \left(\frac{7}{4} n^2 m\ V\right) \frac{(T_o/T_m)^{3/2}}{\sqrt{1-(T_o/T_m)^{7/2}}} \tag{16}$$

where V is the volume of the loop; n_m and T_m are the density and temperature at the loop apex (the minimum and maximum value resp.); and the subscript "o" indicates that the variable is to be evaluated at the time $t = 0$. By using (16) as the initial profile, the physical situation that is being investigated corresponds to that of a flare loop that is initially cooling by conduction, but then radiation cooling begins to dominate and, hence, the temperature profile changes. The evolution of the profile and of the differential emission measure is calculated below.

Using (11), (12a) and (15) the plasma equations reduce to:

$$\frac{\partial n}{\partial t}(s,t) = 0 \tag{17a}$$

$$\frac{3}{2}\frac{\partial}{\partial t} p(s,t) = -n^2 \Lambda(T) \tag{17b}$$

and the equation of state, (5).

Assuming a simple power law form for the radiative losses:

$$\Lambda(T) = LT^{-\ell} \tag{18}$$

where L and ℓ are constants, equation (17) can be solved analytically to yield T(s,t):

$$T(s,t) = T_o(s) \left[1 - \frac{(1 + \ell)\ t}{\tau_r(T_o)}\right]^{1/\ell+1} \tag{19}$$

where $\tau_r(T_o)$ is the radiative cooling time, equation (7), for plasma at temperature T_o:

$$\tau_r(T_o) = \left(\frac{6k^2}{P_o L}\right) (T_o(s))^{-\ell-2} \tag{20}$$

The differential emission measure, equation (1), can now be determined. Expressed as a function of T and t it is given by:

$$Q(T,t) = \frac{Q_o(T_o)\ T^{\ell+1}}{T_o^{\ell+1}[1 + t/\tau_r(T_o)]} \tag{21}$$

where T_o is also considered as a function to T and t, and is obtained by solving equation (19) for $T_o(T,t)$.

In Figure (1), Q is plotted as a function of T/T_m at the times t = 0 and t_1 and for the value of ℓ = 1.5. This is a somewhat larger value for ℓ than is currently accepted (e.g., Rosner et al. 1978), however, we selected it so that the effect of radiative cooling could be clearly visible in the figure. The time t_1 was chosen so that the maximum temperature has decreased by 10% from its initial value, i.e., $T(s_m, t_1)$ =

$.9\ T_o(s_m) = .9\ T_m$, where s_m is the position of the loop apex.

As noted previously, the initial profile $Q_o(T_o)$ has a value of $\delta = 1.5$, except near the singular point $T_o = T_m$ where δ becomes infinite. This singularity has no physical significance (it does not mean that the intensity of lines formed at this temperature are infinite); it simply reflects the mathematical fact that at a temperature maximum the temperature gradient vanishes and, hence, the transformation from s to T implicit in the definition of Q, equation (1), is no longer valid. The emission measure Q cannot be used to calculate line intensities near these temperatures, one must use the temperature and density profiles directly. If this is done, one notes no significant deviation from the $Q_o \propto T_o^{1.5}$ relation, e.g., Underwood et al. (1978).

It is evident from the figure that radiative cooling can produce a steep emission measure profile, at least, for the value of $\ell = 1.5$. The curve for $Q(T,t_1)$ indicates that $\delta(t_1) = 2.5$ except near the singular point $T = .9\ T_m$. This result can be obtained directly from equations (19) and (21). For $T(s,t_1)/T_o(s) \ll 1$, i.e., after a significant amount of cooling has occurred, equation (19) implies that $T_o(T,t)$ is approximately independent of T and, thus, equation (21) implies that $Q(T,t_1) \propto T^{\ell+1}$. On the other hand for $T(s,t_1)/T_o(s) \approx 1$, i.e., for material that has cooled very little, then equations (19) and (21) imply that $Q \approx Q_o$ as expected. Although at $t = t_1$ the hottest plasma has a temperature only 10% less than its initial value, material at lower temperatures have cooled relatively much more due to the strong temperature dependence of the radiative cooling time, equation (20). For example, the plasma with temperature $T(t_1) = 10^{-1}\ T_m$ had an initial temperature of $T_o \approx .7\ T_m$. Thus, the condition that $T(s,t_1)/T_o(s) \ll 1$ is valid for all temperatures except, again,

for a negligibly small interval near the maximum. We conclude, therefore, that for static radiative cooling the steepness of the differential emission measure is given by $\delta = \ell + 1$.

2.3 Isobaric Radiative Cooling

Under assumptions (11) and (12b) the plasma equations become:

$$\frac{\partial n}{\partial t} + \frac{\partial nv}{\partial s} = 0 \tag{22a}$$

$$\frac{\partial p}{\partial s} = 0 \tag{22b}$$

and

$$\frac{3}{2}\frac{\partial p}{\partial t} + \frac{5}{2}\frac{\partial pv}{\partial s} = -n^2\Lambda(T) \tag{22c}$$

Using the approximation for the radiative losses (18), the set above may be combined to yield a single equation:

$$\frac{1}{5p}\frac{dp}{dt}\left[(2\ell + 7)\left(\frac{\partial y}{\partial s}\right)^2 - 2(\ell + 2)\, y\frac{\partial^2 y}{\partial s^2}\right] + \frac{Lp}{10k^2}\left[\frac{1}{y}\left(\frac{\partial y}{\partial s}\right)^2 + (\ell + 2)\frac{\partial^2 y}{\partial s^2}\right] + \frac{\partial y}{\partial t}\frac{\partial^2 y}{\partial s^2} - \frac{\partial^2 y}{\partial t \partial s}\frac{\partial y}{\partial s} = 0 \tag{23}$$

where y is defined as,

$$y \equiv T^{\ell+2} \tag{24}$$

Equation (23) is too complex to solve generally for arbitrary initial conditions; however, particular solutions may be obtained by separation of variables. Letting,

$$y(s,t) = T(0,0)^{\ell+2} \; \theta(t) \; \xi(s), \tag{24}$$

and

$$P(t) = P_o \, \phi(t), \tag{25}$$

equation (23) reduces to:

$$\frac{5 \, T_o}{3 \, \phi} \frac{d\Theta}{dt} \left(\xi \frac{d^2\xi}{ds^2} - \frac{d\xi^2}{ds} \right) + \frac{T_o \, \Theta}{3 \, \phi^2} \frac{d\phi}{dt} \cdot$$

$$\left[(2\ell + 7) \frac{d\xi^2}{ds} - 2(\ell + 2) \, \xi \frac{d^2\xi}{ds^2} \right] + (\ell + 2) \frac{d^2\xi}{ds^2} + \frac{1}{\xi} \frac{d\xi^2}{ds} = 0 \tag{26}$$

where

$$\tau_o = \frac{3/2 \; P_o}{n^2(S_m,0) \; \Lambda(T(S_m,0))} \tag{27}$$

is the initial radiative cooling time scale of the hottest plasma.

A two parameter family of solutions for (26) can be obtained by setting the two time dependent factors to constants. Three equations result: two coupled first order equations which can be integrated completely to yield the time dependence of the temperature and pressure (i.e., $\Theta(t)$ and $\phi(t)$), and one second order equation which can be integrated once to yield the differential emission measure (i.e., $\frac{d\xi}{ds}$ as a function of ξ). The solutions to (26) are:

$$\Theta(t) = (1 + \eta t)^{-\nu} \tag{27a}$$

$$\phi(t) = (1 + \eta t)^{-\nu-1} \tag{27b}$$

$$\frac{d\xi}{ds} = (1+\mu)^{-g(\nu)} \frac{d\xi}{ds}(0) \cdot \xi^{-1/\ell+2} (\xi+\mu)^{g(\nu)} \tag{28}$$

where μ and ν are the two arbitrary parameters, and g and η are given by:

$$g(\nu) = \frac{3(1+\nu)}{(2\ell-1)\nu + 2\ell + 4} + \frac{\ell+3}{\ell+2} \tag{29}$$

and

$$\eta = \frac{3(\ell+2)}{((2\ell-1)\nu + 2\ell + 4)\mu\ \tau_o} \tag{30}$$

Equation (28) can be integrated (at least numerically) to yield the temperature profile; however, we are more interested in expressing the emission measure profile as a function of temperature since that is the observed quantity. Letting T_s be the spatial dependence of the temperature,

$$T_s \equiv \xi(s)^{1/\ell+2} \tag{31}$$

yields:

$$Q(T,t) = \frac{n^2(0,0)}{\frac{dT_s}{ds}(0)} \cdot \Theta(t)^{\frac{2}{2+\nu}-\frac{2}{\ell+2}} \cdot T_s^{\ell+1} \left(\frac{T_s^{\ell+2}+\mu}{1+\mu}\right)^{-g(\nu)} \tag{32}$$

Equation (34) is the main result of the isobaric model. We wish to determine whether a steep dependence of Q on T can be obtained for particular values of the parameters μ and ν. It is evident from (32) that the steepest dependence is obtained if

$$|\mu| << T_s^{\ell+2} \text{ and } g(\nu) < 0 \tag{33}$$

Since in that case, $Q \sim T_s^{\ell+1+(\ell+2)|g|}$. But, it is shown below that (33) implies physically unacceptable solutions.

Using (22), the velocity can be related to the temperature gradient; viz,

$$v \frac{dT_s}{ds} = - \frac{3}{5T_o\mu} \Theta^{1/\nu} T_s^{-\ell-1} (T_s^{\ell+2} + \mu) \tag{34}$$

In order that the velocity be directed opposite to the temperature gradient; i.e., material moves <u>downward</u> as observed, we require,

$$v \frac{dT_s}{ds} < 0 \tag{35}$$

Now, assuming that $|\mu| < T_s^{\ell+2}$ implies we must have $\mu>0$ so that (35) is consistant with (34). However, we also require that the temperature and pressure, $\Theta(t)$ and $\phi(t)$, decrease in time, i.e., the plasma is cooling. From (27), (30) and that μ is positive, this requirement implies that either

$$\nu > 0 \text{ and } (2\ell-1)\nu + 2\ell+4 > 0 \tag{36a}$$

or

$$\nu < -1 \text{ and } (2\ell-1)\nu + 2\ell+4 < 0 \tag{36b}$$

But, if either case (36a) or 36b) is valid, $g(\nu)$ must be positive, equation

(29). Therefore, a physically acceptable solution with $|\mu| < T_s^{\ell+1}$ is not possible unless $g > 0$, which is contrary to what is required, (33), for a steep profile.

From the discussion above it is evident that the only solutions of interest are those with $|\mu| > T_s^{\ell+2}$. In that case, $Q \simeq T_s^{\ell+1}$ over almost all the range of T_s. To illustrate this point the dependence of Q on T_s, i.e., $T_s^{\ell+1}\ (T_s^{\ell+2} + \mu)^{-g}$, is plotted in Figure 2 as a function of T_s for the particular parameters: $\ell = 1.5$, $\mu = -2$ with $\nu = -2$, and $\mu = 1$ with $\nu = 1$ near the singular point $T_s = -\mu$. We note that just as in the static radiative model, $\delta = 2.5$ except near the temperature maximum at $T_s = 1$.

III. DISCUSSION

The main result of the previous section is that for radiatively dominated cooling of corona and transition-region flare plasma the differential emission measure $Q \propto T^{\ell+1}$ and, hence, $\delta = \ell + 1$. It appears unlikely that this dependence can account for the observations which imply $\delta \gtrsim 3$. Calculations of the radiative loss coefficient $\Lambda(T)$ originally did indicate a large value for ℓ in the range $10^6 \lesssim T \lesssim 10^7$ K, e.g., Cox and Tucker's (1969) results indicate $\ell \approx 1.8$. However, these authors did not include the contribution from Fe ions to the radiative losses. More recent calculations (e.g., Tucker and Koren 1971, Raymond et al. 1976) have tended to yield increasingly smaller values for ℓ due to the strong Fe lines formed in the 10^6 - 10^7 K temperature interval. One of the most recent results gives $\delta = .5$, Rosner et al. (1978) and, thus $\delta \approx 1.5$ which is no larger than that predicted by conductive cooling models.

Therefore, we conclude that the proposal of Underwood et al. (1978) is incorrect; radiative cooling cannot produce the steep emission measure profile observed in some flares. On the other hand, the conductive models are also inadequate. There are several possible explanations for the discrepancy. One is that the calculations of predicted line intensities and of $\Lambda(T)$ are inappropriate for flare plasma; however, this does not seem likely. The calculations assume that the plasma is optically thin, is in ionization equilibrium and has standard abundances. Although one or more of these assumptions may be violated during the primary heating phase, they should hold for the long-lived decay phase.

Another possibility is that flare heating is responsible for the steep

profile. However, in that case strong heating would have to continue well into the observed decay phase and have a very specific dependence on density and temperature in order to reproduce the observations.

We believe that the most likely explanation (assuming the observations are not simply due to instrumental error), is that the models developed so far are inappropriate. Various assumptions have been made; the main one being that all plasma velocities are subsonic. This assumption is common to both radiative models considered here, and to the conductive dominated models, (Antiochos and Sturrock 1976, 1978). Supersonic velocities have been observed in cooling flare plasma, but only at low temperatures ($\lesssim 10^{5.5}$ K), below those for which the emission measure profile exhibits a steep dependence (see Underwood et. al. 1978). However, velocities are difficult to observe in higher temperature plasma so that large velocities may be consistant with the data. We intend to investigate flare decay models with supersonic velocities in a subsequent paper, (Antiochos and Sturrock 1979).

ACKNOWLEDGEMENTS

In carrying out this research the author has derived considerable benefit from his participation in the Skylab Solar Workshop on solar flares. The Workshops are sponsored by NASA and managed by the High Altitude Observatory, National Center for Atmosphere Research. This work was performed under NASA contracts NAS8-32263, NGL 05-020-272 and NGR 05-020-559.

REFERENCES

Antiochos, S.K., 1979, SUIPR Number 790.

Antiochos, S.K. and Sturrock, P.A., 1979, (in preparation).

Antiochos, S.K. and Sturrock, P.A., 1978, Ap. J., 220, 1137.

Antiochos, S.K. and Sturrock, P.A., 1976, Solar Phys., 49, 359.

Cox, D.P. and Tucker, W.H., 1969, Ap. J., 157, 1157.

Craig, I.J.D. and Brown, J.C., 1976, Astron. Astrophys., 49, 239.

Culhane, J.L., Vesecky, J.F. and Phillips, K.J.H., 1970, Solar Phys., 15, 395.

Dere, K.P. and Cook, J.W., 1979, Ap. J., 229.

Dere, K.P., Horan, D.M. and Kreplin, R.W., 1977, Ap. J., 217, 976.

Jordan, C., 1976, Phil Trans. Roy. Soc. Lond., A281, 391.

Moore, R.L. and Datlowe, D.W., 1975, Solar Phys., 43, 189.

Moore et. al., 1979, in P.A. Sturrock (ed.), "Solar Flares," Chapter 8, Colo. Assoc. Univ. Press.

Raymond, J.C., Cox, D.P., and Smith, B.W., 1976, Ap. J., 204, 290.

Rosner, R., Tucker, W.H., and Vaiana, G.S., 1978, Ap. J., 220, 643.

Spitzer, L., 1962, "Physics of Fully Ionized Gases," (New York: Wiley Interscience), Chapter 5.

Tucker, W.H. and Koren, M., 1971, Ap. J., 168, 283, and 170, 621.

Underwood, J.H., Antiochos, S.K., Feldman, U. and Dere, K.P., 1978, Ap. J., 224, 1017.

Underwood, J.H. and McKenzie, D.L., 1977, Solar Phys., 53, 417.

Widing, K.G., 1979, (in preparation).

Withbroe, G.L., 1977, Proceedings of the OSO-8 Workshop, University of Colorado, November 1-10.

FIGURE CAPTIONS

1. Graph of log Q versus log $(T(s,t)/T_m)$ for the value of $\ell = 1.5$. The solid curve refers to the time $t = 0$, i.e. the initial emission measure profile, and the broken curve to the later time, $t = t_1$.

2. Graph of the spatial dependence of log Q, i.e. log $[T_s^{\ell+1}(T_s^{\ell+2} + \mu)^{-g}]$, versus log T_s for two isobaric radiative models with $\ell = 1.5$. The solid curve refers to the case with $\mu = 1$ and $\nu = 1$, and the broken to the case with $\mu = -2$ and $\nu = -2$.

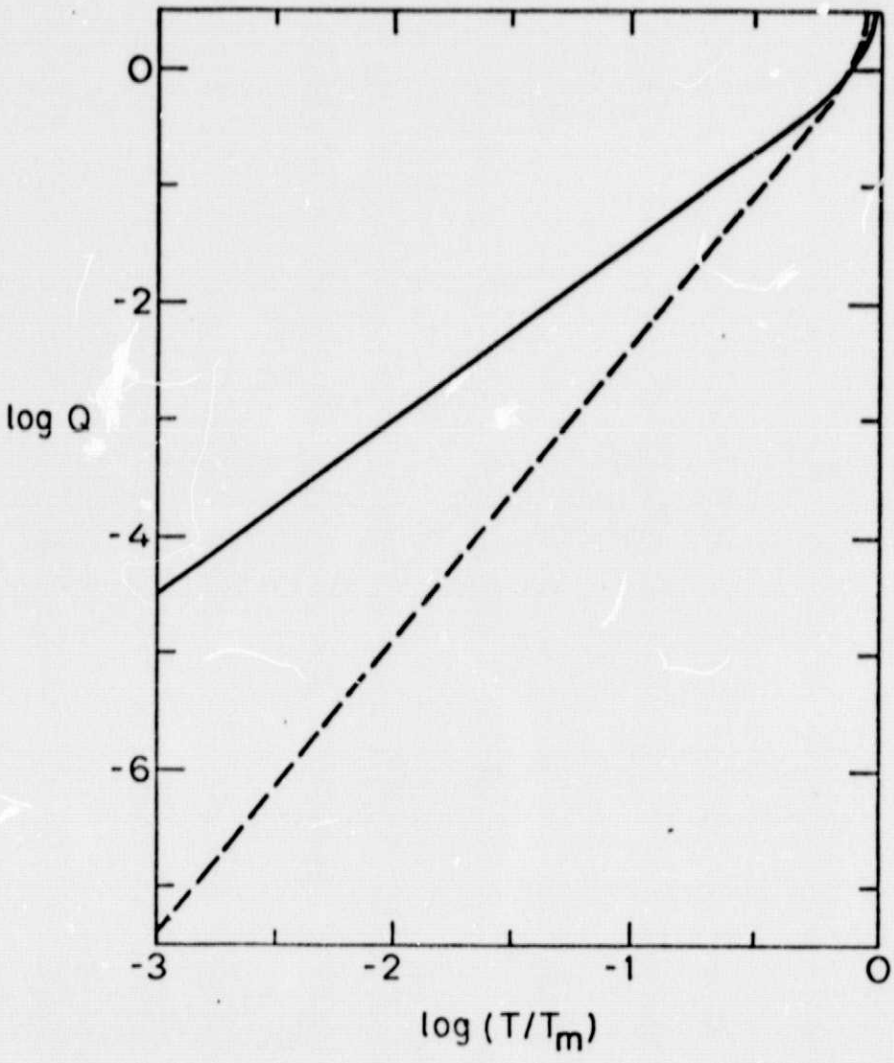

Figure 1

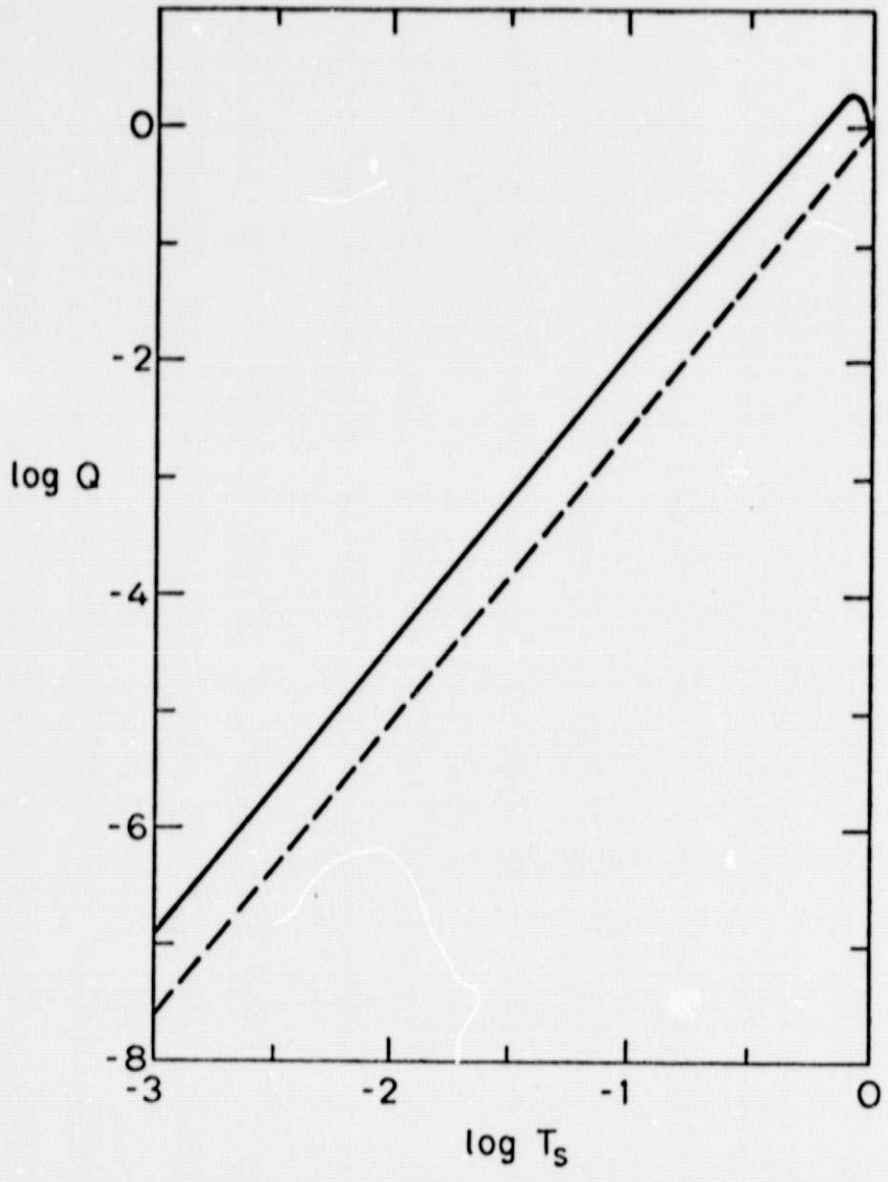

Figure 2